Designing a Low-Temperature Scattering-type Near Field Optical Microscope

Julie Cass
University of Notre Dame

ABSTRACT

The goal of this project was to design a scattering-type scanning near field optical microscope (s-SNOM) to probe samples for optical, topographical and chemical information at a wide range of temperatures and under vacuum conditions. The instrument is implemented with a parabolic mirror to achieve improved focusing and collection of scattered light with a shear force atomic force microscope (AFM) controlling tip-sample distance. Electronics required for the AFM included driving and detecting circuits to excite the AFM tuning fork and amplify the signal from its oscillation while obtaining the greatest signal-to-noise ratio possible.

INTRODUCTION

The scattering-type scanning near field optical microscope (s-SNOM) is designed to overcome the diffraction limit of classical microscopes in order to study samples on the nanometer scale. It employs an electrochemically etched metal tip simultaneously for optical scattering and as a probe for an atomic force microscope (AFM). Evanescent waves in the sample near field carry spectral and spatial information about the sample. The s-SNOM method uses the metal tip to localize light in this near field and scatter evanescent waves into the far field for optical detection and analysis [1]. In this simple implementation the system can be used for chemical analysis called tip-enhanced Raman spectroscopy (TERS) [2]. Raman spectroscopy uses inelastic light scattering to obtain a chemical fingerprint of a sample from vibrational properties. In TERS, the tip's ability to localize the light field and enhance scattering both can be used to enhance this Raman signal, achieving single molecule sensitivity [3].

The tip can also function as an AFM probe to control tip-sample separation. We implemented a shear force AFM, using the damping effects of the shear force on a tuning fork as a feedback mechanism to maintain the tip-sample distance [4]. The metal tip is brought close to the sample and raster scanned parallel to the sample surface. A feedback loop is used to maintain a constant separation distance between the tip and sample, keeping the tip close to the sample without making contact in order to achieve maximum optical enhancement. Information from this tip scan could also be used to obtain a topographical map of the sample surface [1].

The goal of placing this system in low temperature and vacuum is to study how the optical properties of materials change under those conditions. Previous experiments have been done to probe samples with shear force, however these experiments usually employed a traditional lens as the focusing agent for their designs and did not implement low temperature systems. We plan to improve on this design by implementing a parabolic mirror as the focusing agent in order to increase the amount of scattered light collected and the precision with which the light is focused. Studies have been done implementing a parabolic mirror but only under ambient conditions [3]. Our microscope would combine these elements along with a circuit system designed for the greatest possible signal-to-noise ratio to achieve a microscope with greater signal and light collection efficiency that can operate under low temperatures and in vacuum.

Implementing a microscope under these conditions causes great complication in the system design. Many electrical components do not function well at low temperatures and many materials cannot be used in vacuum. This strictly limits the components that can be used inside the chamber. It is also necessary to have remote control of the objects inside it, as the chamber is isolated to maintain its low temperature.

THE AFM DESIGN

1. The Shear Force

The effects of s-SNOM are optimized when the sample is kept close to the AFM tip without making

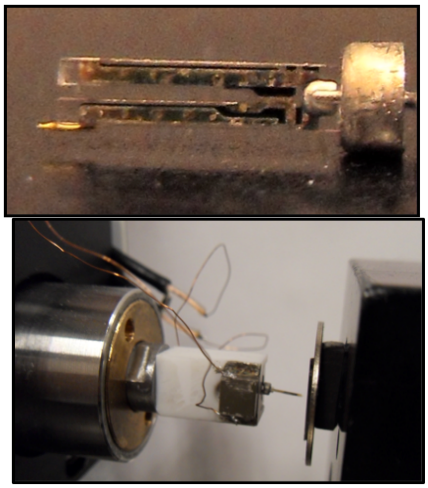

FIGURE 1a. Metal tip mounted to commercial quartz tuning fork 1b. Tuning fork and tip (center) approaching sample (right)

contact with it. The shear force AFM was developed to use the effect of the shear force on small tuning forks as a feedback mechanism for controlling this tip-sample distance. The sample is moved on a piezo stage, raster scanned in parallel to the sample surface and kept close to the AFM tip according to the feedback loop. The metal tip of the AFM is mounted to a small Auris commercial tuning fork with dimensions of about 4.60mm x 1.75mm x 1.05mm and a small electrode in each tine. The tuning forks are designed to have a resonance frequency of about 32.768 kHz, however this will deviate slightly from one tuning fork to the next. While in their packaging casings, these tuning forks often have a quality factor of about 30,000, but this Q-factor drops by about 10,000 when the packing is removed [5]. One of these tuning forks is photographed in Figure 1a.

The tuning forks are made of quartz, which is a piezoelectric material. When voltages are applied to such materials, they react by distorting slightly, on the nanometer scale. When alternating voltages are applied to the inner electrodes of the tuning fork, they can be piezoelectrically driven to oscillate, causing the tip to vibrate parallel to the sample surface. However, as the tip and tuning fork are brought very close to the sample, as in Figure 1b, the oscillation is damped. This effect is called the shear force [3].

This force is not entirely understood, however it is believed to either be an effect of van der Waals forces or viscous damping from a thin water layer on the sample surface [1]. A graph of the change in oscillation amplitude as the tip approaches the sample is given in Figure 2. The amplitude

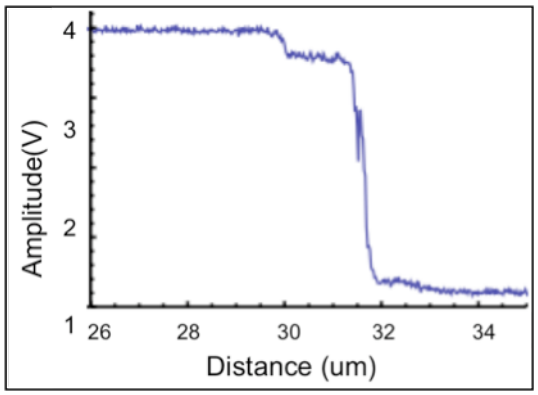

FIGURE 2. Approach curve. The oscillation amplitude is damped as the sample approaches and makes contact with tip.

difference between this damped signal and the reference signal from the function generator can be used as an indication of the proximity of the tip to the sample. The signal from the tuning fork and the reference signal are sent into a lock-in amplifier. The lock-in signal is sent to a PID, which uses the difference between these signals to adjust the z-piezo, communicating how it must adjust to maintain a constant tip-sample distance. This PID system allows the system to respond quickly to variations in topography, maintaining a close tip-sample approach without allowing the two to make contact.

This AFM system can be implemented for optical studies when light is applied to achieve a near field signal. Light is focused onto this tip-sample interface using a parabolic mirror and the scattered light is recollected and redirected out, parallel to the tip. It could then sent to a camera or spectroscope for analysis.

2. Focusing with a Parabolic Mirror

We implemented a parabolic mirror with numerical aperture of approximately 1 to focus and recollect scattered light from the AFM. Two different orientations for the mirror were discussed. The first consisted of the sample sitting in the bottom of the mirror with the mirror parabola extending up away from the sample. Light would be directed downward into the mirror while the AFM head is suspended over the sample inside the mirror. Alternatively, we discussed positioning the mirror with the tip protruding through a hole in the center of the mirror and the sample sitting below, under the dome of the mirror [3]. After much debate it was determined that this second orientation would be optimal based on the simplicity of the setup, total light collection and

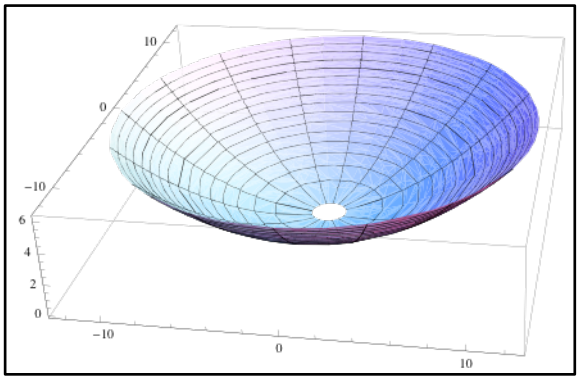

FIGURE 3. A Mathematica representation of the parabolic mirror to be implemented in the shear force AFM

surface area of mirror needed. As the system will be placed within the confines of a cryostat it was important to consider the amount of space the different mirror orientations would require.

In order for the desired field enhancements to occur, the electric field must be lined along the axis of the AFM tip [6,3]. In addition, focusing the incoming light beam requires that it be lined up precisely with mirror's optical axis, so it is important to have good control of the beam path. This will be achieved using high precision steering optics located outside the chamber.

A Mathematica representation of this mirror and schematic of light scattering are given in Figures 3 and 4. The parabolic mirror was designed to have a diameter of 25mm and a focal length of 6.25 mm, such that the edge of the mirror is even with the focal point. This creates an angle of collection from the center of the mirror to its edge of a full 90 degrees, to ensure that all scattered light is collected. Classically, SNOM set-ups use an objective lens to focus light on the sample and collect the scattered light. We chose to implement a parabolic mirror for its much higher solid angle of light collection [3]. Figure 4 allows for a visual comparison of how these focusing agents are implemented. The hole through the center of the mirror for the tip does slightly decrease the solid

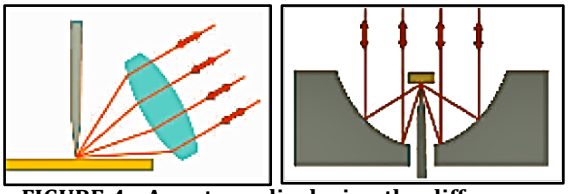

FIGURE 4. A cartoon displaying the difference between using a lens and a parabolic mirror in solid angle of light collection

angle of light collection, but this the majority of this incoming illumination is already blocked by the sample. Thus adding the hole in the mirror for the tip does not significantly decrease the solid angle of light collection.

There are numerous other benefits to choosing to use a parabolic mirror rather than an objective for light focusing and collection. While objectives have a focal plane, the parabolic mirror provides a single tight focal point [7]. Ideally, all light scattered from a parabolic mirror passes through this point and can be reflected in a perfect parallel beam. This degree of precision requires that the mirror be very smooth, with a surface roughness less than a tenth wavelength. Furthermore the parabolic mirror is given a silver coating for high reflectivity over visible wavelengths.

CIRCUIT DESIGN

The complete design for the driving and detection circuitry of this AFM in standard conditions is given in Figure 5. The circuitry for the AFM under low temperature and vacuum is slightly different, as certain components of the circuit under standard conditions will not hold or function under the desired low temperatures or vacuum. To account for this adjustments and an additional component must be added to the low temperature circuit, discussed later in this paper.

The main purpose of the circuit is to efficiently drive the tuning fork oscillation and amplify the

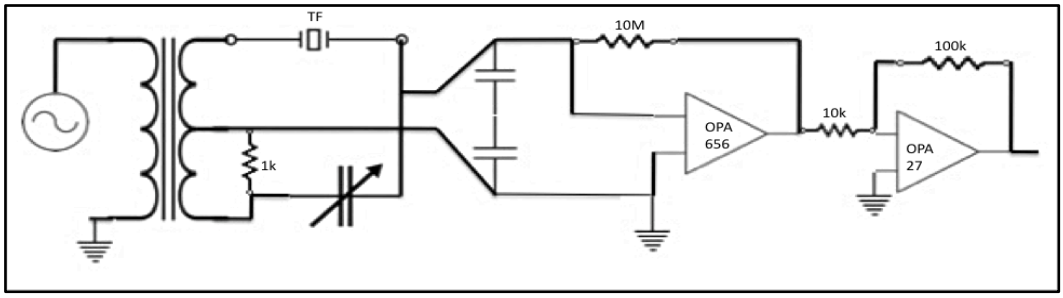

FIGURE 5. An electronic diagram of the circuitry implemented for the driving of the tuning fork oscillation and detecting of the resulting signal

signal using the detection circuit. Several methods for implementing this were discussed in an effort to select the excitation method with greatest signal-to-noise ratio. This is particularly important for our design due to the use of long cables carrying stray capacitance and the large number of connections needed in the chamber. Analysis of Jahncke's study entitled "Choosing a Preamplifier for Tuning Fork Signal Detection in Scanning Force Microscopy" in *Review of Scientific Instruments* was of particular importance in the task [8]. The paper outlines the advantages and disadvantages of driving a tuning fork mechanically and electrically and with a voltage or current preamplifier, ranking the four possible combinations by signal-to-noise ratio.

While the study determined the combination of the voltage amplifier and mechanical drive (voltage OPA-655) to be the have the greatest signal to noise ratio (79) [8] we determined that the use of a dither piezo to mechanically drive our system would not be preferable. The additional piezo adds bulk to the design that could block laser light and add additional vibrations to the system. As a result, we elected to use the system found to have the second highest signal to noise ratio (65): the electrically driven oscillation with current preamplifier (current OPA-655) [8]. This became the basis for our design of the driving and detecting circuits.

1. The Driving Circuit

Before beginning any experiments with the AFM, the resonant frequency of the tuning fork must be found. While all the tuning forks in a set will have roughly the same resonant frequency, the addition of the tip and slight variations between tuning forks makes determining each individual fork's resonance necessary. This was done using the sweep mode on a function generator to drive the tuning fork [9]. This applies a sinusoidal wave (voltage) at a constantly increasing frequency, from one specified frequency up to another. This causes the tuning fork to oscillate at this varying frequency.

We monitored the amplitude of the oscillation using Labview, graphing the amplitude as a function of driving frequency. This produces a Lorentzian curve, with the peak amplitude being the amplitude at resonance. A sample graph of this Lorentzian relationship with the resonance is given in Figure 5. By collecting this data and considering the frequency at the peak amplitude, we can determine the resonant frequency with which we should drive the AFM circuit. We can see that for different tuning forks the resonant frequency will vary from the 32.768 kHz figure given by the company. For example, the tuning fork in Figure 6 has a resonance close to 32.785 kHz. The width of the peak of the Lorentzian for each tuning fork is related to each tuning fork's Q factor.

This circuit is designed to drive the oscillation of the tuning fork while working to cancel out imperfections in the fork vibration caused by what is called shunt capacitance, making an improvement over previous implementations of similar microscopes. The tuning fork can be described in terms of an equivalent circuit consisting of a resistor, inductor and capacitor all in series with one another, and in parallel with a second capacitor. [4]. This parallel capacitor represents the shunt capacitance in the fork, an imperfection that causes a distortion in the line shape of the parallel RLC resonance.

An example of this is visible in Figure 6. Here the sample data collected from running a frequency sweep on the tuning fork is fitted with a Lorentzian curve. Upon closer investigation we can see that the data falls consistently above the Lorentzian on one side of the resonant peak and below it on the other. This asymmetry is one example of a distortion caused by the tuning fork shunt capacitance. To cancel out these effects the circuit employs a center-tapped transformer and variable capacitor.

To begin the driving circuit, the wave function generator is set to send out sine waves at the previously described resonant frequency. This signal is then sent through the center-tapped transformer, which splits the signal into two waveforms phase shifted from one another by 180 degrees (while the center tap is grounded) [8]. One of these waves is directed through a variable capacitor. The signal through this variable capacitor is used to cancel out the effects of the shunt capacitance as it interferes with the signal from the

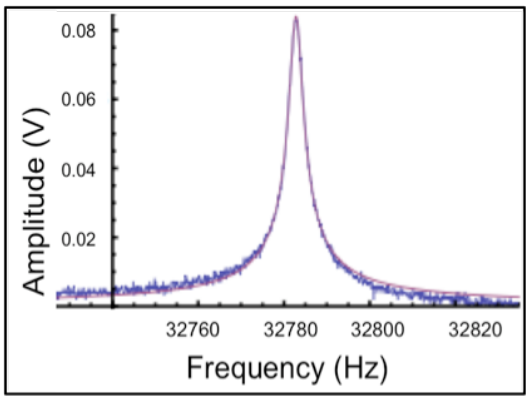

FIGURE 6. Sample frequency sweep for finding resonant frequency fitted with a Lorentzian curve

tuning fork [9]. These two wave signals will essentially cancel each other out, leaving only the pure resonance of the RCL equivalent circuit. The second wave is used to electrically drive the tuning fork oscillation.

The AC voltage signal is sent into one of the tuning fork electrodes causing the fork to piezoelectrically expands and contract, the second tine oscillating towards and away from the driven one [5]. This induces a current in the second electrode, which is then sent out into the circuit. We selected this means of driving the tuning fork because it allows us to use the electric-drive/current preamplifier combination that we determined to be best suited for our experiment. We avoided the use of a bulky dither piezo and produced a current signal rather than a voltage.

The end result of this circuit is to have the tuning fork oscillating at the desired resonant frequency (for optimized signal) without the distorting effects to its oscillation of its internal shunt capacitance. The circuit produces the desired current signal, which can be sent to the detection circuit for amplification.

2. The Detection Circuit

The goal of the detection circuit is to convert the current signal from the tuning fork back into a voltage and amplify it. The output signal from the tuning fork is extremely small and dissipates quickly due to the stray capacitance in the wires of the system [8]. It was therefore important to both minimize the distance that the signal must travel through the wires to reach an amplifier and that we have the greatest signal-to-noise ratio possible. While the current preamplifier in the paper was an OPA-655, we elected to use an upgraded version of the preamplifier (OPA-656) that has since been developed.

We began by designing a detection circuit for an AFM that is under standard conditions. The signal is first sent to the OPA-656, an operational amplifier that works to convert the signal from a current to a voltage while also amplifying it [9]. This op-amp is connected in parallel with a resistor, which controls the noise in the signal and helps to preserve its line shape and control amplifier gain. The signal then goes to a second operational amplifier called an OPA-27, which is used to simply to further amplify the signal. The OPA-656 differs from the OPA-27 in that it is designed for particularly low noise generation. This is important, as the OPA-656 is the first stage amplifier for the signal. It is important that this component amplify the signal for the rest of the detection circuit without distorting it with its own generation of electrical noise. Otherwise this noise would be integrated into the signal and amplified when the signal is sent to the OPA-27, distorting the signal even further.

The detection circuit for the AFM in low temperature and vacuum, however, will be slightly different. The OPA-656 cannot operate under these conditions and must be placed outside of the cryostat. However the signal still dissipates quickly and an amplifier must still be placed very close to it, inside the cryostat. For this purpose we must add a MESFET, a type of transistor that can be used to provide a first-stage amplification inside the chamber, before passing the signal outside of the chamber to the detection circuit [9].

CONCLUSION

The design for this system is not yet complete, but much progress was made during the summer. One main focus of this summer was to determine the orientation of the mirror and how the AFM head, parabolic mirror and sample would be placed together. In addition decisions about how to drive and detect the signal of the tuning fork electronically with the greatest signal-to-noise ratio was of upmost importance. The project will continue with further advancement in the cryogenic design and decisions of how to optimally support and connect the various components of the system within the narrow cryostat to create an instrument with highest precision.

ACKNOWLEDGEMENTS

I would like to thank Markus Raschke for his advisement and inclusion of me in his research group for the summer. I would also like to thank Joanna Atkin for her tremendous advising, guidance and partnership in this project. Also, thanks to Emily Chavez for her partnership in the project, especially the design of our circuits and development of our sample AFM. Finally, thanks to Sam Berweger and the rest of the Raschke group for their additional mentoring and to Subhadeep Gupta and Alejandro Garcia for their coordination of the INT Physics REU program.

REFERENCES

[1] C. Neacsu, Ph.D. Dissertation, University of Washington, 2008.

[2] Kharinstev, *Nanotechnology* **18**, 315502 (2007).

[3] B. Pettinger, *Review of Scientific Instruments* **78**, 103104 (2007).

[4] K. Karrai, *Review of Scientific Instruments* **71**, 2776 (2000).

[5] Nanonis GmbH, "Piezoelectric Tuning Forks for Scanning Probe Microscopy," 2005. www.nanonis.com

[6] A. Meixner, *Journal of Micrscopy* **229**, 247 (2008).

[7] A. Meixner, *Optics Letters* **33**, 681 (2008).

[8] C. L. Jahncke, *Review of Scientific Instruments* **75**, 2759 (2004).

[9] Paul Horowitz and Winfield Hill, *The Art of Electronics*, 2nd ed. (Cambridge University Press, New York), 1989.